observed effects resulted from orthodromic activation of FEF neurons with top-down projections to posterior visual areas[22], including direct projections to V4 as well as to parietal and temporal areas, this is only one of many possible ways in which stimulation could gate signals in area V4. Future experiments should aim to specify further the pathway or pathways that are sufficient to bring about the observed gain modulation.

Primate vision consists of a sequential sampling of the details contained within a scene[23]. The extraction of information from a scene depends on the continual shifting of perceptual resources, such as the foveas, across locations in space. This process must include the reciprocal interaction of brain mechanisms that are involved primarily in coding the visual stimulus with those that are involved primarily in moving the eye[24]. The results of the current study reveal an equivalence of biases in oculomotor preparation and biases in the gain of spatially corresponding visual signals when oculomotor plans are not carried out. As such, covert spatial attention may simply reflect one emergent property of visuomotor integration. □

## Methods

We recorded the responses of V4 cells to oriented-bar stimuli while the monkey fixated a central spot and while subthreshold stimulation trains lasting 20–50 ms (200 Hz, biphasic, 0.2-ms pulse duration) were applied to the FEF. We determined the metrics of the evoked saccade and the movement threshold of each FEF site in a separate behavioural paradigm in which stimulation with varying current amplitude was delivered to the site during the performance of a fixation task[8]. During the experiment, visual stimuli (50–93% Michaelson contrast) were presented for 1.5–2 s inside and outside the RF of a V4 neuron. RFs were mapped in a further behavioural paradigm in which oriented bars were swept across the display during fixation while monitoring the activity of the recorded cell[25]. Bar stimuli were presented either at the preferred orientation or orthogonal to the preferred orientation during successive trials. All visual stimuli were displayed on a video monitor (30 cm vertical × 40 cm horizontal, 60 Hz) positioned 57 cm in front of the monkey. Throughout behavioural testing, eye position was monitored through a scleral search coil and stored at 200 Hz. All general surgical and experimental procedures, which have previously been described[26], were approved by the Princeton University Animal Care and Use Committee and were in accordance with National Institutes of Health guidelines.

Received 15 October; accepted 25 November 2002; doi:10.1038/nature01341.


1. Sperling, G. & Melchner, M. J. The attention operating characteristic: examples from visual search. *Science* **202,** 315–318 (1978).
2. Blaser, E., Sperling, G. & Lu, Z. L. Measuring the amplification of attention. *Proc. Natl Acad. Sci. USA* **96,** 11681–11686 (1999).
3. Moran, J. H. & Desimone, R. Selective attention gates visual processing in the extrastriate cortex. *Science* **229,** 782–784 (1985).
4. Haenny, P. E. & Schiller, P. H. State dependent activity in monkey visual cortex. I. Single cell activity in V1 and V4 on visual tasks. *Exp. Brain Res.* **69,** 225–244 (1988).
5. Motter, B. C. Focal attention produces spatially selective processing in visual cortical areas V1, V2, and V4 in the presence of competing stimuli. *J. Neurophysiol.* **70,** 909–919 (1993).
6. Desimone, R. & Duncan, J. Neural mechanisms of selective visual attention. *Annu. Rev. Neurosci.* **18,** 193–222 (1995).
7. Rizzolatti, G., Riggio, L., Dascola, I. & Umilta, C. Reorienting attention across the horizontal and vertical meridians: evidence in favor of premotor theory of attention. *Neuropsychologia* **25,** 31–40 (1987).
8. Moore, T. & Fallah, M. Control of eye movements and spatial attention. *Proc. Natl Acad. Sci. USA* **98,** 1273–1276 (2001).
9. van Hooff, J. A. R. A. M. in *Non-Verbal Communication* Ch. 7 (ed. Hinde, R. A.) Ch. 7 (Cambridge Univ. Press, Cambridge, UK, 1972).
10. Shepherd, M., Findlay, J. M. & Hockey, R. J. The relationship between eye movements and spatial attention. *Q. J. Exp. Psychol. A* **38,** 475–491 (1986).
11. Hoffman, J. E. & Subramaniam, B. The role of visual attention in saccadic eye movements. *Percept. Psychophys.* **57,** 787–795 (1995).
12. Tehovnik, E. J., Sommer, M. A., Chou, I. H., Slocum, W. M. & Schiller, P. H. Eye fields in the frontal lobes of primates. *Brain Res. Brain Res. Rev.* **32,** 413–448 (2000).
13. Bruce, C. J., Goldberg, M. E., Bushnell, M. C. & Stanton, G. B. Primate frontal eye fields. II. Physiological and anatomical correlates of electrically evoked eye movements. *J. Neurophysiol.* **54,** 714–734 (1985).
14. Penfield, W. & Rasmussen, T. *The Cerebral Cortex of Man: A Clinical Study of Localization of Function* (Macmillan, New York, 1950).
15. Godoy, J., Luders, H., Dinner, D. S., Morris, H. H. & Wyllie, E. Versive eye movements elicited by cortical stimulation of the human brain. *Neurology* **40,** 296–299 (1990).
16. Schiller, P. H. & Tehovnik, E. J. Look and see: how the brain moves your eyes about. *Prog. Brain Res.* **134,** 127–142 (2001).
17. Burman, D. D. & Bruce, C. J. Suppression of task-related saccades by electrical stimulation in the primate's frontal eye field. *J. Neurophysiol.* **77,** 2252–2267 (1997).
18. Moore, T., Tolias, A. S. & Schiller, P. H. Visual representations during saccadic eye movements. *Proc. Natl Acad. Sci. USA* **95,** 8981–8984 (1998).
19. Schall, J. D., Morel, A., King, D. J. & Bullier, J. Topography of visual cortex connections with frontal eye field in macaque: convergence and segregation of processing streams. *J. Neurosci.* **15,** 4464–4487 (1995).
20. Leopold, D. A. & Logothetis, N. K. Microsaccades differentially modulate neural activity in the striate and extrastriate visual cortex. *Exp. Brain Res.* **123,** 341–345 (1998).
21. McAdams, C. J. & Maunsell, J. H. R. Effects of attention on orientation-tuning functions of single neurons in macaque cortical area V4. *J. Neurosci.* **19,** 431–441 (1999).
22. Stanton, G. B., Bruce, C. J. & Goldberg, M. E. Topography of projections to posterior cortical areas from the macaque frontal eye fields. *J. Comp. Neurol.* **353,** 291–305 (1995).
23. Yarbus, A. L. *Eye Movements and Vision* (Plenum, New York, 1967).
24. Moore, T. Shape representations and visual guidance of saccadic eye movements. *Science* **285,** 1914–1917 (1999).
25. Zipser, K., Lamme, V. A. F. & Schiller, P. H. Contextual modulation in primary visual cortex. *J. Neurosci.* **16,** 7376–7389 (1996).
26. Nakamura, K., Chung, H. H., Graziano, M. S. & Gross, C. G. Dynamic representation of eye position in the parieto-occipital sulcus. *J. Neurophysiol.* **81,** 2374–2385 (1999).


**Acknowledgements** We thank C. G. Gross and M. Fallah for their help. This work was supported by grants from the National Institutes of Health, and a HHMI predoctoral fellowship to K.M.A.

**Competing interests statement** The authors declare that they have no competing financial interests.

**Correspondence** and requests for materials should be addressed to T. M. (e-mail: tirin@princeton.edu).

# Pivotal role of oligomerization in expanded polyglutamine neurodegenerative disorders

**Ivelisse Sánchez*†, Christian Mahlke* & Junying Yuan***

** Department of Cell Biology, Harvard Medical School, Boston, Massachusetts 02115, USA*

**The expansion of a CAG repeat coding for polyglutamine in otherwise unrelated gene products is central to eight neurodegenerative disorders including Huntington's disease[1]. It has been well documented that expanded polyglutamine fragments, cleaved from their respective full-length proteins, form microscopically visible aggregates in affected individuals and in transgenic mice[2–7]. The contribution of polyglutamine oligomers to neurodegeneration, however, is controversial. The azo-dye Congo red binds preferentially to β-sheets containing amyloid fibrils[8,9] and can specifically inhibit oligomerization[10] and disrupt preformed oligomers. Here we show that inhibition of polyglutamine oligomerization by Congo red prevents ATP depletion and caspase activation, preserves normal cellular protein synthesis and degradation functions, and promotes the clearance of expanded polyglutamine repeats *in vivo* and *in vitro*. Infusion of Congo red into a transgenic mouse model of Huntington's disease, well after the onset of symptoms, promotes the clearance of expanded repeats *in vivo* and exerts marked protective effects on survival, weight loss and motor function. We conclude that oligomerization is a crucial determinant in the biochemical properties of expanded polyglutamine that are central to their chronic cytotoxicity.**

To assess directly the role of oligomerization in the cytotoxicity of expanded polyglutamines, we determined whether anti-amyloid compounds that are known to bind to β-sheet-containing amyloid fibrils, including polyanions[11], tetracyclines[12] and azo-dyes such as Congo red[8,10] and chrysamine G[13], could prevent expanded poly-

† Present address: Department of Anatomy and Neurobiology, Boston University School of Medicine, 715 Albany Street, L-813, Boston, Massachusetts 02118, USA.

glutamine induced cell death (Fig. 1). We transfected HeLa cells with an expression construct encoding an expanded polyglutamine tract tagged with haemagglutinin A (HA–Q79). As shown previously, the expression of Q79 resulted in cell death (Fig. 1a), detectable 48 h after transfection[14]. Congo red, but none of the other agents tested, showed a remarkable protective effect (60%) against cell death induced by HA–Q79 (Fig. 1a). Given these results, we examined the specific effects and mechanism by which the β-sheet-binding compound Congo red exerts protection against polyglutamine-induced toxicity.

Changes in energy metabolism have been detected in brain tissue from presymptomatic animal models of, and presymptomatic individuals with, Huntington's disease[15]. We detected a sharp decrease in concentrations of ATP on expression of expanded polyglutamine in cells, which reached close to minimal levels as early as 24 h after transfection (Fig. 1b–d). This ATP depletion, however, was inhibited by the addition of zVAD.fmk, a polycaspase inhibitor, suggesting that changes in the energy metabolism leading to the reduction in ATP take place downstream of caspase activation (Fig. 1b). Congo red significantly inhibited the loss of ATP induced by expression of expanded polyglutamine in a time- and dose-dependent manner (Fig. 1c, d). Addition of Congo red 6 h after transfection prevented ATP depletion. A reduced but detectable protective effect was also achieved when Congo red was added as late as 24 h after transfection, a time when aggregated, expanded polyglutamine was already visible in untreated control cells (Fig. 1c). An additive effect of two doses (6 and 24 h) of Congo red on the preservation of ATP concentrations was seen (Fig. 1c). No general increases in ATP were detected in control cells treated with Congo red (Fig. 1b).

Inhibition of general protein synthesis is an important early event in cell death[16]. To determine whether Congo red inhibits the loss of protein synthesis in cells expressing polyglutamine, we co-transfected HeLa cells with a luciferase construct and HA–Q79, and determined protein synthesis by luciferase activity 48 h after transfection. Expression of HA–Q79 led to a significant loss of luciferase expression. Treatment with Congo red prevented the reduction in luciferase activity, as well as ATP loss and cell morphological changes, in a similar dose-dependent manner (Fig. 1d).

To verify that Congo red exerts a protective effect on general protein synthesis in Q79-expressing cells, we determined the amounts of newly synthesized protein by a [$^{35}$S]methionine pulse-chase experiment. In agreement with data from the luciferase assay, treatment with Congo red prevented the decrease in newly synthesized $^{35}$S-labelled proteins in Q79-expressing cells specifically, but had no effect on the basal amounts of protein synthesis in cells expressing green fluorescent protein (GFP) or in control primary neurons (Fig. 1e and Supplementary Fig. 1a, b). These results indicate that Congo red does not function as a general ATP or protein synthesis enhancer but exerts specific effects upstream to inhibit the loss of cellular functions.

As expanded polyglutamine repeats can recruit and activate caspase-8 (ref. 14), we tested whether treatment with Congo red inhibits the activation of caspase-8 as well as a downstream caspase, caspase-3, in Q79-expressing cells (Fig. 1f, g). HeLa cells were transfected with HA–Q79 in the presence or absence of Congo red, and the cell lysates were analysed by western blot. The appearance of an active caspase-8 fragment of relative molecular mass 45,000 ($M_r$ 45K) was detected at 24 h, preceding the extensive morphological changes but concurrent with the timing of ATP loss (Fig. 1f and Supplementary Fig. 2). Addition of Congo red completely inhibited the appearance of active caspase-8 induced by Q79 expression and consequently also the appearance of activated caspase-3 (Fig. 1g). The inhibition of Q79-induced caspase activation by Congo red was also shown by a fluorogenic general caspase substrate: addition of Congo red or caspase inhibitor zVAD.fmk prevented the appearance of zVAD–FITC-positive cells (Fig. 1h). Consistent with this result, lysates from HA–Q79 expressing cells that had been cultured in the presence of Congo red showed considerably less caspase-8 and -3 activity than did samples treated with PBS (Fig. 1i, bottom).

To determine whether Congo red could inhibit the ability of expanded polyglutamine aggregates to activate caspases independently of cellular metabolic activity, we established a cell-free system with recombinant glutathione *S*-transferase (GST)-tagged Q19 or Q81 in the presence of HeLa cell S100 lysate and IETD.AFC, a fluorogenic substrate for caspase-8 like activity (Fig. 1i, top). The presence of GST–Q81 but not GST–Q19 in HeLa S100 lysate

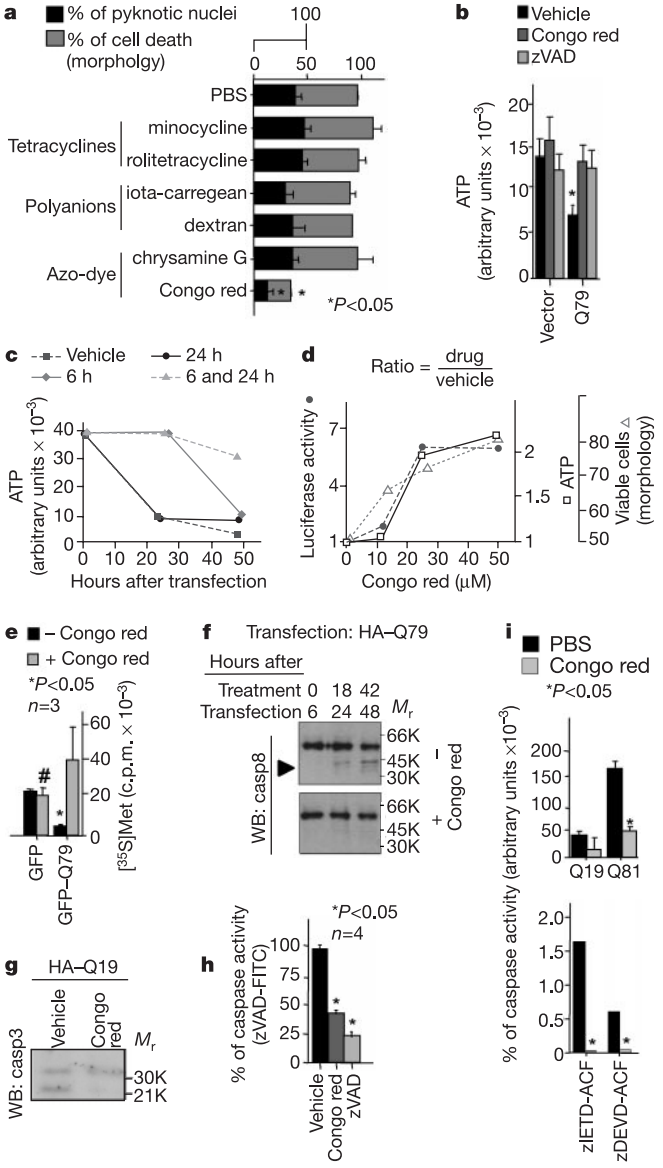


**Figure 1** Effect of anti-amyloid compounds on cell death induced by polyglutamine. **a**, Percentage of cell death in HeLa cells expressing HA–Q79 treated with the indicated compounds (100 μM) for 42 h starting at 6 h after transfection. **b**, **c**, ATP concentrations in control or HA–Q79-transfected HeLa cells and in cells treated with 100 μM Congo red (100 μm), zVAD (100 μm) or PBS for 42 hrs (**b**) or at the indicated number of hours after transfection (**c**). **d**, Dose-dependent effects of Congo red. **e**–**i**, Effects of Congo red on protein synthesis assessed by [$^{35}$S]methionine labelling (**e**), on activation of caspase-8 and caspase-3 (**f**, **g**), and on caspase activity in cells using a zVAD–FITC assay (**h**), in a cell-free system using zIETD.AMC (**i**, top) or in cells lysates using zIETD.AMC or zDEVD.AMC (**i**, bottom).

induced the activation of caspase-8 like activity. Notably, Congo red inhibited the activation of caspase activity in this cell-free system in which the contribution of the proteasome was ruled out by the use of MG132. This experiment suggests that Congo red can inhibit the activation of caspases induced by expanded polyglutamine independently of cell metabolic activity. Taken together, these experiments show that Congo red can inhibit caspase activation induced by expanded polyglutamine in both cells and a cell-free system, and provide biochemical evidence supporting the proposal that Congo red can alter the biochemical and biophysical properties of expanded polyglutamine that underpin its cytotoxicity.

Because overexpression of heatshock chaperone proteins such as HSP40 and HSP70 has been shown to inhibit cell death[17,18] and seems to alter the properties of polyglutamine oligomers[19,20], we determined whether Congo red induced an increase in the expression of endogenous chaperones. Congo red treatment of cells expressing HA–Q79 had no effect on the expression of HSP40 or HSP70 (Supplementary Fig. 2). Thus, Congo red is unlikely to act indirectly through induction of chaperone proteins. In addition, a possible direct inhibitory effect of Congo red on the cell death machinery was ruled out as Congo red did not inhibit any of the pro-apoptotic and necrotic stimuli tested (Supplementary Fig. 3).

Although Congo red did not block the general cell death machinery, it showed an obvious inhibitory effect on the aggregation of expanded polyglutamine, concurrent with its inhibitory effect on cell death (Fig. 2). When SH-SY5Y neuroblastoma cells were treated with Congo red 6 h after transfection with Q79 tagged with GFP (Q79–GFP), the formation of expanded polyglutamine aggregates was reduced significantly (Fig. 2a). In addition, incubation of the semipurified polyglutamine aggregates with Congo red but not with any of the other compounds resulted in the dissolution of preformed aggregates (Fig. 2b). Thus, Congo red can inhibit nucleation as well as disrupt preformed expanded polyglutamine aggregates.

We designed a chemical absorption assay that measures the remaining compound in the supernatant after incubation with GST–polyglutamine beads and their subsequent removal by centrifugation. The amyloid-like conformation of GST–Q81 and GST–Q62 was confirmed by fluorescence microscopy after staining with Thioflavin T (data not shown). Congo red had a significantly higher affinity to expanded polyglutamine (Q81 and Q62) than to polyglutamine with 19 repeats (Q19) at equal protein concentrations (Fig. 2c), suggesting that Congo red does not bind to polyglutamine *per se*, but interacts with the specific conformation of expanded polyglutamine. Thus, Congo red can differentiate between expanded and normal-length polyglutamine.

To confirm further the ability of Congo red to inhibit polyglutamine oligomerization and to disrupt preformed aggregates, we analysed the state of polyglutamine aggregation by examining equal aliquots of total lysates from cells expressing HA–Q79 that had been treated with Congo red or vehicle, or lysates that were treated with Congo red or vehicle after cell lysis. Cell lysates were passed through a 0.2-μm acetate filter membrane and the Q79 remaining on the filter membrane was visualized after immunostaining with antibodies against HA (Fig. 2d). HA immunoreactivity for Q79 on the filters was undetectable from lysates isolated from cells treated with Congo red for 48 h starting at 6 h after transfection or from lysates treated with Congo red for 30 min after cell lysis (Fig. 2d). This indicates that Congo red can both inhibit the formation of poly-

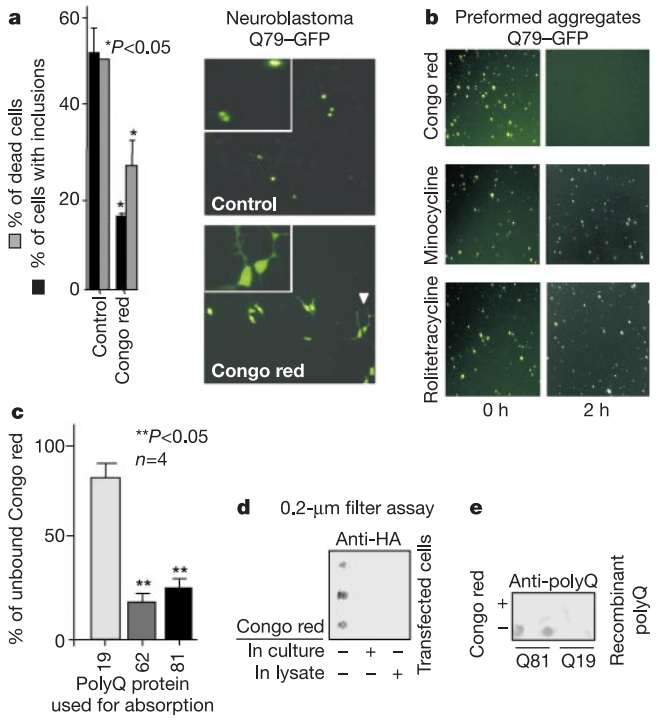


**Figure 2** Selective inhibition of polyglutamine oligomerization and cytotoxicity by Congo red. **a**, Cell death and polyglutamine oligomerization in SH-SY5Y cells expressing Q79–GFP treated with 100 μM Congo red or PBS for 42 h starting at 6 h after transfection. **b**, Lysates from Q79-expressing cells were treated with 100 μM of indicated compounds (2 h) and visualized by fluorescence microscopy. **c**, Preferential binding of Congo red to Q81 and Q62 rather than Q19, as determined by chemical absorption assay (*$P < 0.01$). **d**, **e**, Effect of Congo red on preformed oligomers (**d**) or on purified recombinant GST–Q19 or GST–Q81 as determined by the filter assay using EM48 antibodies (**e**).

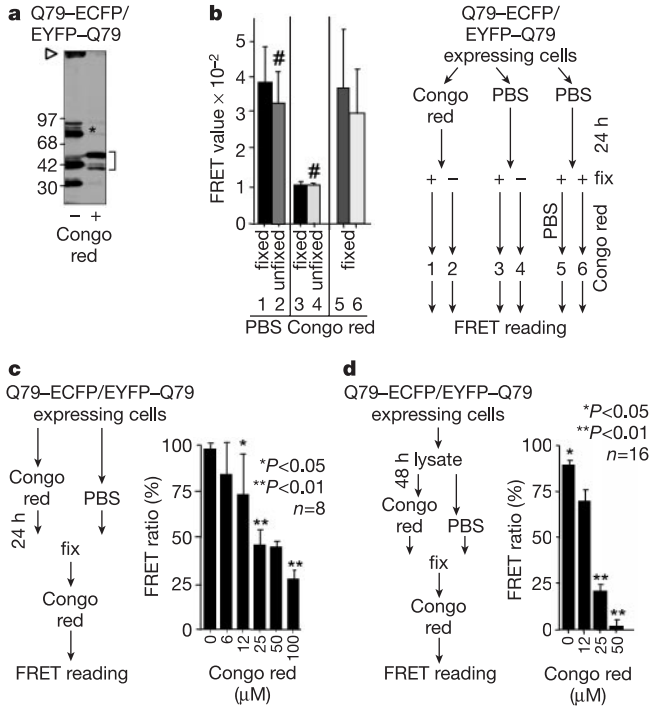


**Figure 3** FRET assay for polyglutamine oligomerization. **a**, Western blot of lysates from cells expressing EYFP–Q79 and Q79–ECFP and treated with Congo red (+) or PBS (−) were probed with antibodies against ECFP and EYFP. Open arrowhead indicates the insoluble aggregates at the top of gel. **b**, No significant difference on FRET value occurred after fixation with 1% PFA. **c**, **d**, Dose-dependent effect of Congo red on formation of Q79 oligomers in cells (**c**) and disruption of preformed oligomers from cell lysates (**d**), as determined by FRET.

glutamine aggregates (at least larger than 0.2 μm in size) in cells and dissolve preformed polyglutamine aggregates.

We confirmed that Congo red can inhibit aggregate formation in the absence of other cellular proteins by carrying out the filter assay with bacterially expressed and purified recombinant Q81 and Q19 incubated with either vehicle or 100 μM Congo red (Fig. 2e). In contrast to Congo red, compounds such as chrysamine G, which is structurally very similar to Congo red and can bind expanded polyglutamine aggregates (data not shown), did not disrupt the formation, dissolve preformed polyglutamine aggregates or inhibit cell death induced by expanded polyglutamine in our assays (Fig. 1). These results indicate that the ability of Congo red to inhibit and disrupt polyglutamine oligomerization but not binding *per se* is crucial to the inhibition of cell death induced by expanded polyglutamine repeats.

To rule out the possibility that Congo red merely disrupts the large polyglutamine aggregates without affecting the formation of oligomeric polyglutamine units, which may be indistinguishable by conventional fluorescent microscopy, we used a fluorescence resonance energy transfer (FRET) Q79 assay. Enhanced yellow fluorescent protein (EYFP)-tagged Q79 and enhanced cyan fluorescent protein (ECFP)-tagged Q79 were co-transfected into HeLa cells (Fig. 3a). On western blot with antibodies against EYFP/ECFP, lysates from cells transfected with HA–Q79–ECFP and EYFP–HA–Q79 but untreated with Congo red showed several high $M_r$ bands including SDS-insoluble HA–Q79–ECFP and EYFP–HA–Q79 aggregates unable to enter the separating gel (Fig. 3a, arrowhead) and oligomers that entered the gel (Fig. 3a, asterisk). By contrast, lysates from cells treated with Congo red contained two protein bands close to the predicted $M_r$ for HA–Q79–ECFP and EYFP–HA–Q79 on SDS polyacrylamide gel electrophoresis (SDS–PAGE; ref. 21 and Fig. 3a, brackets).

The oligomeric interaction of expanded polyglutamine in cells was examined further by FRET between HA–Q79–ECFP and EYFP–HA–Q79 24 h after their transfection into cells cultured in the presence or absence of Congo red (Fig. 3b–d). The value of FRET was determined as the ratio between fluorescence at 535 nm and that at 460 nm after excitation at 430 nm. To exclude the effect of Congo red absorption, we defined the ratio of FRET as the value of FRET in cells treated with Congo red divided by the maximum FRET in control cells to which Congo red was added after fixation. To determine the maximum value of FRET, we co-transfected cells with HA–Q79–ECFP and EYFP–HA–Q79, and 24 h after transfection we fixed them with 1% paraformaldehyde. Congo red was added after fixation and the value of FRET was determined as mentioned above and used as a 100% control value for each concentration of Congo red used. Fixation by 1% paraformaldehyde *per se* had no effect on FRET (Fig. 3b). Cells cultured in the presence of Congo red (6–50 μM) were also fixed with 1% paraformaldehyde 24 h after transfection, and Congo red was then added to the original treatment concentration to normalize for absorption effects. Treatment with Congo red caused a dose-dependent inhibition of the FRET ratio between Q79–ECFP and EYFP–Q79, indicating that Congo red can inhibit Q79 oligomerization (Fig. 3c).

To verify the ability of Congo red to disrupt preformed oligomers independently of cellular function, we determined the effect of Congo red on isolated polyglutamine aggregates by FRET (Fig. 3d). Cells transfected with HA–Q79–ECFP and EYFP–HA–Q79 were lysed, treated with Congo red or PBS, and fixed with 1% paraformaldehyde. The FRET value and ratio were determined as above in the presence of Congo red after fixation. Preformed Q79 oligomers were also disrupted by Congo red, as indicated by the dose-dependent decreases in FRET after Congo red treatment (Fig. 3d). These experiments confirm that Congo red can inhibit the formation of, as well as disrupt, preformed polyglutamine oligomeric units independently of cellular function.

To examine whether disruption of polyglutamine oligomerization interferes with its interaction and the concurrent aggregation of other proteins, we co-transfected cells with Q79 and one of the following expression constructs, GFP–FADDdn, GFP–caspase-8dn or GFP-tagged to exon 1 of the *huntingtin* gene (HDQ25–GFP), in the presence of Congo red or zVAD.fmk. Congo red but not zVAD.fmk clearly prevented the recruitment and aggregation of GFP–FADDdn, GFP–caspase-8dn and HDQ25–GFP (Fig. 4a, b). Congo red treatment also prevented the recruitment of endogenous FADD, or caspase-8 by expanded polyglutamine aggregates, as shown by the 0.2-μm filter assay (Fig. 4c). These results underscore the selectivity of Congo red on the oligomeric expanded polyglutamine repeats and its inhibitory effects on the subsequent downstream events, including aberrant protein–protein interactions and aggregation.

Because these expanded polyglutamine oligomers accumulate in cells and seem to have a significantly slower turnover rate than that of shorter polyglutamine[22], we tested the effect of Congo red on the turnover of Q79 oligomers by measuring the amounts of [$^{35}$S]methionine pulse-labelled polyglutamine. The quantities of newly synthesized Q79 1 h after chase were higher in cells treated with Congo red than in untreated cells, clearly showing that Congo red does not suppress the expression of Q79 (Fig. 5a, top). But the amounts of $^{35}$S-labelled HA–Q79 were over twofold less after 24 h of pulse chase in cells treated with Congo red, suggesting that there is a faster turnover rate of HA–Q79 in the presence of Congo red than in its absence (Fig. 5a, top, and 5b). In line with these results, the steady-state quantities of Q79 were more than twofold less after 24 h in the presence of Congo red than in its absence (Fig. 5a, bottom).

As we had already determined that Congo red does not function as a general enhancer of protein synthesis (Fig. 1), we wanted to rule out the possibility that Congo red may affect general protein degradation by testing its effect on proteasome-mediated protein degradation. Whereas protein degradation was inhibited by the general proteasome inhibitor MG132, Congo red or zVAD had no effect on general protein degradation (Supplementary Fig. 4). To test whether inhibition of Q79 aggregation also prevents the reported inhibition in proteasome activity[23,24], we measured the

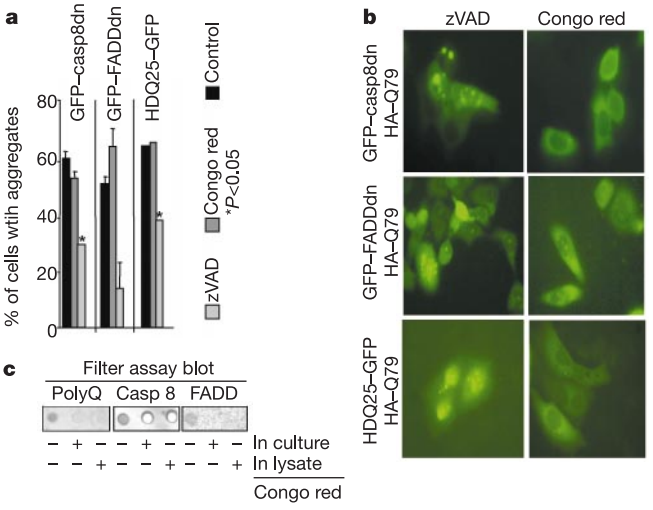


**Figure 4** Inhibition of polyglutamine oligomerization prevents abnormal protein recruitment. **a**, **b**, Effect of Congo red on the recruitment by Q79 of GFP-tagged caspase-8dn, FADDdn and huntingtin Q25 in the HeLa cells. Cells co-transfected with HA–Q79 and one of the indicated constructs above were pretreated with 100 μM zVAD.fmk or 100 μM Congo red. **c**, Lysates from cells expressing HA–Q79 treated with 100 μM Congo red or PBS alone in culture or after lysis were passed through a 0.2-μm filter. The presence of expanded polyglutamine aggregates, endogenous caspase-8 and FADD in the filter was detected by EM48 antibodies, antibodies against caspase-8 or antibodies against FADD, respectively.

relative degradation of proteasome substrates z-LLE-AMC and suc-LLVY-AMC (Fig. 5c, d). Cells transfected with HA–Q79 were treated with PBS or Congo red and lysed 24 h after transfection in the presence of the fluorogenic substrate with or without the addition of MG132 (10 μM). Congo red treatment ameliorated the Q79-induced inhibition of proteasome activity (Fig. 5c, d). This indicates that, although Congo red has no direct effect on the basal cellular protein degradation, it most probably promotes the clearance of expanded polyglutamine aggregates by increasing its accessibility to cellular protein degradation machinery, by maintaining cellular ATP and protein synthesis, and by restoring the function of ubiquitin–proteasome pathway, which is inhibited on expression of polyglutamine repeats[23,24].

To examine further the cellular fate of expressed HA–Q79, we analysed the distribution of soluble HA–Q79 in cells incubated with or without Congo red after high-speed centrifugation by sucrose gradients. When proteins from control cells expressing HA–Q79

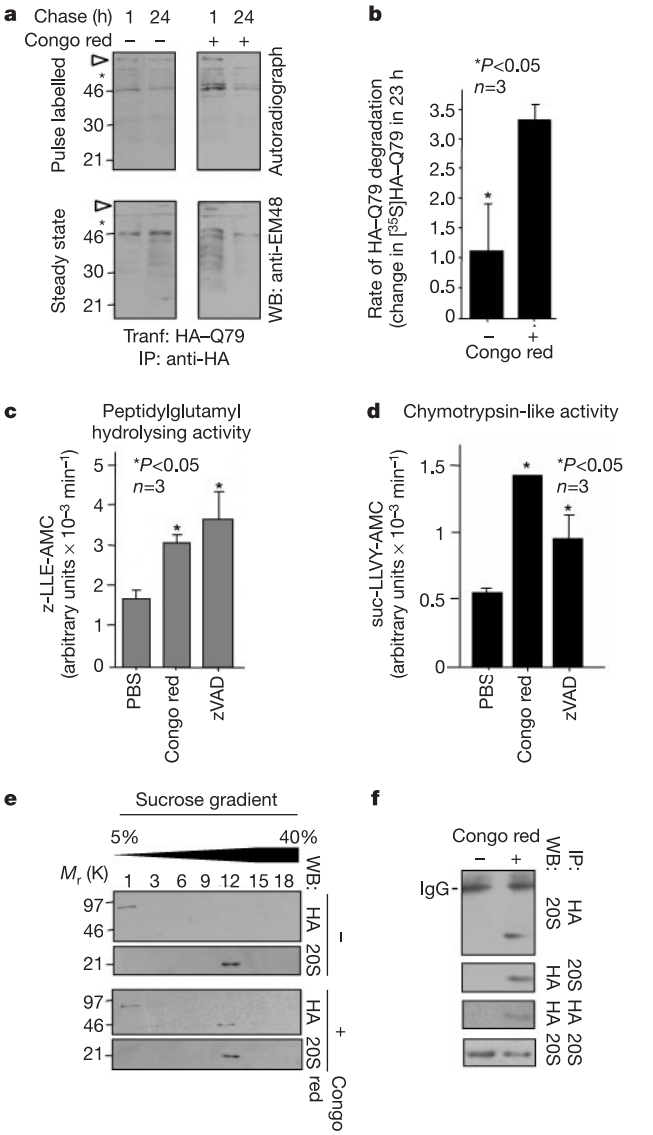


**Figure 5** Effect of Congo red on polyglutamine turnover. **a**, Cells expressing HA–Q79 were labelled with [$^{35}$S]methionine for 1 h and chased for 24 h, and then anti-HA immunoprecipitates were analysed by autoradiography (top) or EM48 antibodies (bottom). **b**, Amounts of $^{35}$S-labelled polyglutamine protein in cells with (+) or without Congo red (−) treatment determined in three experiments as described in **a**. Values are the means ± s.d. **c**, **d**, Proteasome activity was measured with (+) or without (−) Congo red using zLLE-AMC (**c**) and suc-LLVY-AMC (**d**). **e**, High-speed supernatants from cells expressing HA–Q79 and treated with (+) or without (−) Congo red were fractionated by sucrose gradient and analysed by western blot using antibodies against HA or 20S (alpha type-1 proteasome subunit). **f**, Proteins from sucrose gradient fraction 12 were immunoprecipated with antibodies against HA or 20S subunit to test their interaction.

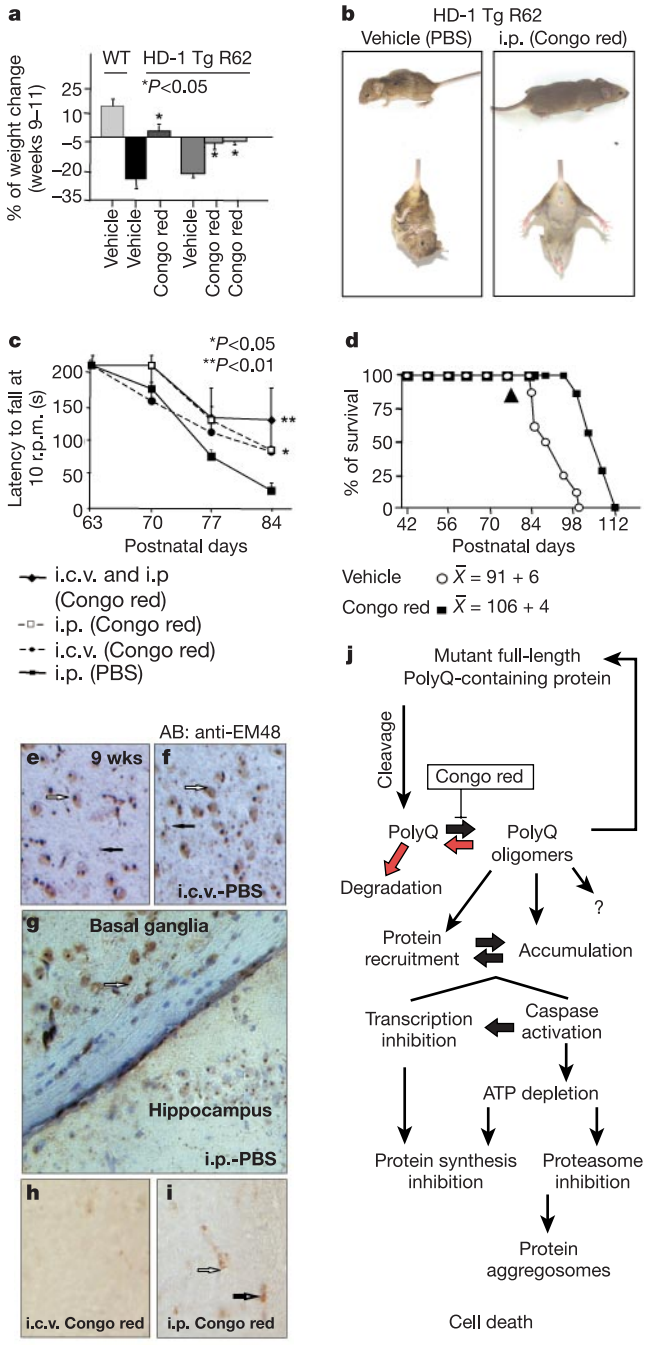


**Figure 6** Effect of Congo red in the transgenic R62 mouse model of Huntington's disease. **a**, **b**, Effect of Congo red on body weight loss (**a**), and overall health aspect and dyskinesia of the hindlimbs at 12.5 weeks of age (**b**). **c**, Latency to fall at 10 r.p.m. on rotarod. Congo red or vehicle treatment was carried out from 9 to 14 weeks of age by i.p. every 48 h ($n = 8$), by i.c.v. pump ($n = 8$), or by both ($n = 4$). **d**, Survival of R62 mice treated with Congo red ($n = 13$) or vehicle ($n = 13$). **e**–**i**, Immunostaining of the basal ganglia of R62 mice at 9 weeks of age (**e**) and brain sections from mice treated with either vehicle (**f**, **g**) or Congo red at 12.5 weeks (**h**, **i**) using EM48 antibodies. **j**, Model of the disruption of polyglutamine oligomerization by Congo red.

were subjected to a 5–40% sucrose gradient, soluble HA–Q79 was detected at the top of the gradient and as a ~90K protein on SDS–PAGE. In samples treated with Congo red, a significant portion of soluble HA–Q79 migrated with a high $M_r$ complex at the bottom half of the gradient and as a ~46K protein on SDS–PAGE (Fig. 5f). Notably, the 20S subunit of proteasome was detected in the same fraction and was coimmunoprecipitated with HA–Q79 in samples treated with Congo red (Fig. 5e). These results suggest that Congo red treatment shifts the equilibrium of soluble expanded polyglutamine from the higher oligomeric form to a lower $M_r$ form that permits it to interact with a high $M_r$ complex containing the 20S proteasome subunit.

To examine directly the role of polyglutamine aggregates on characteristic features of disease progression in expanded polyglutamine disorders, we used the R62 mouse model of Huntington's disease, in which a truncated form of huntingtin with 139 CAG repeats is expressed[7]. Because Congo red can disrupt preformed oligomers, we concentrated on its impact on disease progression after the formation of polyglutamine aggregates and the onset of symptoms. We infused Congo red either at a dose of 1 mg per 30 g (body weight) every 48 h intraperitoneally (i.p.) or through a 28-d intracerebroventricular cannula (i.c.v.; 6 μg every 24 h) starting at postnatal week 9. Infusion of Congo red either i.p. or i.c.v. resulted in no gross morphological abnormalities or induction of any obvious symptoms in normal wild-type mice or in pre- or post-symptomatic R62 mice (data not shown). A common feature of disorders caused by expanded polyglutamine repeats, including Huntington's disease, is severe weight loss as a part of the systemic pathology (Fig. 6a, b). The severe weight loss observed in R62 transgenic mice expressing the expanded polyglutamine repeats was significantly ameliorated after Congo red treatment by either i.c.v. or i.p. delivery (Fig. 6a).

R62 mice also develop severe diabetes owing to the presence of polyglutamine aggregates in the pancreas[25], a feature mimicking the elevated diabetes rate in individuals affected with Huntington's disease[26]. R62 transgenic mice treated with Congo red had significantly reduced blood glucose concentrations ($178 \pm 46\,mg\,dl^{-1}$) as compared with PBS-treated R62 transgenic mice ($398 \pm 98\,mg\,dl^{-1}$) and had similar concentrations to those of wild-type mice treated with either PBS ($152 \pm 27\,mg\,dl^{-1}$) or Congo red ($216 \pm 60\,mg\,dl^{-1}$) after 6 h of fasting. Thus, the treatment of Congo red is effective against both peripheral symptoms of R62 mice.

Initial abnormal neurological signs of R62 mice include dyskinesia of the hindlimbs when mice are suspended by the tail and irregular gait[7]. Treatment with Congo red significantly inhibited the dyskinesia of hindlimbs (Fig. 6b) and preserved normal gait and stride length. Whereas the average stride length of vehicle-treated R62 transgenic mice was decreased by 46% to that of wild type, R62 mice treated with Congo red showed only a 17% reduction in stride length (see Supplementary Fig. 5). The effect of Congo red on motor performance in R62 mice was also assessed by rotarod. R62 mice treated with Congo red preserved their motor function, whereas PBS-treated R62 mice continued to deteriorate (Fig. 6c). The life span of R62 mice was also significantly prolonged by Congo red treatment, resulting in a mean survival length of 106 d as compared with 91 d in vehicle-treated mice (Fig. 6d).

To verify that Congo red could disrupt and inhibit the formation of expanded polyglutamine oligomers *in vivo*, we analysed brain samples from control and Congo-red-treated R62 mice by immunostaining with EM48 antibodies against polyglutamine repeats[27,28]. The basal ganglia of 9-week-old R62 mice showed extensive EM48-positive polyglutamine aggregates as described previously (ref. 7 and Fig. 6e). Extensive clearance of expanded polyglutamine repeats was observed in the basal ganglia of 12.5-week-old mice treated with Congo red but not with vehicle (Fig. 6, compare panels f and g with h and i). A moderate reduction of EM48-positive polyglutamine aggregates was also observed in the hippocampus (data not shown). Thus, *in vivo* Congo red can both disrupt preformed polyglutamine aggregates and inhibit the nucleation of new polyglutamine aggregates.

We conclude that disrupting polyglutamine oligomerization directly inhibits the ability of expanded polyglutamine to induce several cytotoxic events, such as activation of caspases and ATP depletion, providing a mechanism of protection independent of cellular metabolism. At the same time, inhibition of polyglutamine oligomerization facilitates the degradation of expanded polyglutamine by increasing its accessibility to proteasome and thereby indirectly reducing the accumulation of toxic products and preserving the normal cellular metabolic activity (Fig. 6j). Although our studies do not address the role of mutant full-length proteins containing expanded polyglutamine repeats, they indicate that inhibition of polyglutamine oligomerization may provide a viable therapeutic approach for Huntington's disease and other related polyglutamine expansion disorders in which toxic expanded polyglutamine fragments are generated. □

## Methods

### Assays for cellular metabolism

Proteasome activity was determined by using 10 μM suc-LLVY-AMC or Z-LLE-AMC (Alexis) with or without MG132. Fluorescence for AMC (excitation 380 nm, emission 460 nm) in MG132-treated samples was subtracted as background. The luciferase activity was determined in cells expressing HA–Q79– or pcDNA6–luciferase 48 h after transfection using the Steady-Glo substrate and Wallach plate reader (Packard). We determined total protein synthesis from cells expressing HA–Q79–GFP or GFP, or nontransfected primary neurons after a 1-h incubation with [$^{35}$S]methionine and 10 μM MG132 6 h after transfection or after 2 or 7 d after treatment. Proteins were precipitated with 20% trichloroacetic acid and the amount of $^{35}$S was determined using a Beckman LS6000 scintillation counter.

### Fluorometric detemination of caspase activity

Caspase-8-like or caspase-3-like activity was determined by using the AFC-conjugated fluorogenic substrates IETD and DEVD, respectively (Biomol) or *in situ* by the Caspatag kit (Intergen).

### Antibodies

We used the following antibodies: EM48 (ref. 27), antibodies against HSP40 and HSP70 (Stressgen) and a rat monoclonal antibody against caspase-8 (ref. 14). Immunoreactivity was determined with the appropriate horseradish-peroxidase-labelled secondary antibody by ECL (Amersham)

### Chemical absorption assays

We scanned each compound solution between 200 nm and 800 nm using a DU640 spectrophotometer (Beckman) to determine its optimal 'signature wavelength'. The absorbance of Congo red at 460 nm after incubation with glutathione beads alone was used as the 100% value. Purified recombinant GST–Q19, GST–Q62 and GST–Q81 (ref. 29) were diluted to a final concentration of $5\,\mu g\,ml^{-1}$. Compounds tested included Congo red, minocycline, dextran, iota-carregean, rolitetracycline (Sigma) chrysamine G (AG Scientific) or vehicle alone (0.2% dimethyl sulphoxide (DMSO) in PBS).

### Cell-free aggregation and filter assay

HeLa cell lysates were passed through a needle to ensure the release of polyglutamine inclusions from the nuclei. The supernatants were centrifuged twice at 4,000 r.p.m. for 30 s over a 25% sucrose cushion to remove unbroken nuclei. Polyglutamine aggregates were aliquoted into 384-well plates and treated with Congo red, minocycline or rolitetracycline at a final concentration of 0–100 μM. Filter assays were done as described[10]. The HA–Q79–GFP aggregates and recombinant GST–Q19 and GST–Q81 were passed through a 0.2-μm filter and the presence of HA-tagged Q79 or polyglutamine was detected with antibodies against HA or with EM48 antibodies, respectively.

### Immunoprecipitation and protein turnover rates

HeLa cells transfected with a HA–Q79 construct were treated with 100 μM Congo red or PBS 6 h after transfection. Twenty-three hours after transfection, cells expressing HA–Q79 were metabolically labelled in methionine-free DMEM medium containing 50 μCi of [$^{35}$S]methionine (Gibco) in the presence of PBS or 100 μM Congo red for 1 h. We washed cells to remove unincorporated label and chased them for 1 or 24 h before collection. After centrifugation at 2,000*g* for 3 min, the cells were lysed in PBS containing Triton X-100 and protease inhibitors. Sepharose bound to HA antibodies (Babco) was used to immunoprecipitate HA–Q79 from lysates. We processed immunoprecipitates for autoradiography and western blotting with EM48 antibodies. To determine the rates of total cellular protein degradation, $2 \times 10^4$ cells were seeded in 12-well dishes and treated with Congo red (100 μM), zVAD.fmk (100 μM) or MG132 (10 μM) and labelled with $5\,\mu Ci\,ml^{-1}$ [$^3$H]tyrosine for 1 h and the amounts of [$^3$H]tyrosine determined using the LS6000 scintillation counter (Beckman).

### Mice surgery and treatment

We obtained 6-week-old R62 transgenic mice and CBA × C57Bl/6 $F_1$ wild-type littermates from Jackson laboratories. The genotype was confirmed by polymerase chain reaction as described[7]. Mice were treated after 1 week of daily rotarod training. Mice were anaesthetized by intraperitoneal injection of chloral hydrate and osmotic pumps (0.25 μl $h^{-1}$ for 28 d), and the cannula were implanted intracerebroventricularly (Alzet) using predetermined coordinates (anterior/posterior, −0.5 mm, 1 mm lateral to the bregma). Congo red was diluted at 1 mg $ml^{-1}$ in calcium- and magnesium-free PBS plus 0.2% DMSO. The vehicle solution contained 0.2% DMSO in calcium- and magnesium-free PBS. For intraperitoneal injections, 0.5 ml of 1 mg $ml^{-1}$ Congo red in PBS plus 0.2% DMSO was injected every 48 h. The protocol was approved by the Harvard Medical School Standing Committee on Animals.

### Behavioural tests, rotarod performance

Two days after their first treatment, we tested the mice for motor performance and coordination by using a rotarod (Columbus Instruments) at 10 r.p.m. for a maximum of 210 s and by the 'ink' test[30]. The mice were weighed once a week. Two rotarod trials were carried out three times a week in a blind manner.

### Tissue preparation and histology

Mice were anaesthetized with isoflurane and perfused intracardially with 4% paraformaldehyde in PBS. The brain was removed and washed several times in PBS before being incubated overnight in PBS containing 30% sucrose and embedded in OCT (optimal culling temperature) (Sigma) for sectioning. We stained the sections with EM48 antibodies at a dilution of 1:1,000 and detected immunoreactivity with the ABC kit according to the manufacturer's instructions (Vector).

Received 14 August; accepted 6 November 2002; doi:10.1038/nature01301.


1. The Huntington's Disease Collaborative Research Group. A novel gene containing a trinucleotide repeat that is expanded and unstable on Huntington's disease chromosomes. *Cell* **72,** 971–983 (1993).
2. Wellington, C. L. *et al.* Inhibiting caspase cleavage of huntingtin reduces toxicity and aggregate formation in neuronal and nonneuronal cells. *J. Biol. Chem.* **275,** 19831–19838 (2000).
3. Kim, Y. J. *et al.* Caspase 3-cleaved N-terminal fragments of wild-type and mutant huntingtin are present in normal and Huntington's disease brains, associate with membranes, and undergo calpain-dependent proteolysis. *Proc. Natl Acad. Sci. USA* **98,** 12784–12789 (2001).
4. Lunkes, A. *et al.* Proteases acting on mutant huntingtin generate cleaved products that differentially build up cytoplasmic and nuclear inclusions. *Mol. Cell* **10,** 259–269 (2002).
5. Wellington, C. L. *et al.* Caspase cleavage of mutant huntingtin precedes neurodegeneration in Huntington's disease. *J. Neurosci.* **22,** 7862–7872 (2002).
6. Perutz, M. Polar zippers: their role in human disease. *Protein Sci.* **3,** 1629–1637 (1994).
7. Mangiarini, L. *et al.* Exon 1 of the HD gene with an expanded CAG repeat is sufficient to cause a progressive neurological phenotype in transgenic mice. *Cell* **87,** 493–506 (1996).
8. Klunk, W. E., Pettegrew, J. W. & Abraham, D. J. Quantitative evaluation of Congo red binding to amyloid-like proteins with a β-pleated sheet conformation. *J. Histochem. Cytochem.* **37,** 1273–1281 (1989).
9. Carter, D. B. & Chou, K. C. A model for structure-dependent binding of Congo red to Alzheimer β-amyloid fibrils. *Neurobiol. Aging* **19,** 37–40 (1998).
10. Heiser, V. *et al.* Inhibition of huntingtin fibrillogenesis by specific antibodies and small molecules: implications for Huntington's disease therapy. *Proc. Natl Acad. Sci. USA* **97,** 6739–6744 (2000).
11. Caughey, B. & Raymond, G. J. Sulfated polyanion inhibition of scrapie-associated PrP accumulation in cultured cells. *J. Virol.* **67,** 643–650 (1993).
12. Howlett, D. R., George, A. R., Owen, D. E., Ward, R. V. & Markwell, R. E. Common structural features determine the effectiveness of carvedilol, daunomycin and rolitetracycline as inhibitors of Alzheimer β-amyloid fibril formation. *Biochem. J.* **343,** 419–423 (1999).
13. Klunk, W. E., Debnath, M. L. & Pettegrew, J. W. Chrysamine-G binding to Alzheimer and control brain: autopsy study of a new amyloid probe. *Neurobiol. Aging* **16,** 541–548 (1995).
14. Sanchez, I. *et al.* Caspase-8 is required for cell death induced by expanded polyglutamine repeats. *Neuron* **22,** 623–633 (1999).
15. Beal, M. F., Hyman, B. T. & Koroshetz, W. Do defects in mitochondrial energy metabolism underlie the pathology of neurodegenerative diseases? *Trends Neurosci.* **16,** 125–131 (1993).
16. Deckwerth, T. L. & Johnson, E. M. Jr Temporal analysis of events associated with programmed cell death (apoptosis) of sympathetic neurons deprived of nerve growth factor. *J. Cell Biol.* **123,** 1207–1222 (1993).
17. Jaattela, M., Wissing, D., Kokholm, K., Kallunki, T. & Egeblad, M. Hsp70 exerts its anti-apoptotic function downstream of caspase-3-like proteases. *EMBO J.* **17,** 6124–6134 (1998).
18. Wyttenbach, A. *et al.* Effects of heat shock, heat shock protein 40 (HDJ-2), and proteasome inhibition on protein aggregation in cellular models of Huntington's disease. *Proc. Natl Acad. Sci. USA* **97,** 2898–2903 (2000).
19. Chai, Y., Koppenhafer, S. L., Bonini, N. M. & Paulson, H. L. Analysis of the role of heat shock protein (Hsp) molecular chaperones in polyglutamine disease. *J. Neurosci.* **19,** 10338–10347 (1999).
20. Kazemi-Esfarjani, P. & Benzer, S. Genetic suppression of polyglutamine toxicity in *Drosophila*. *Science* **287,** 1837–1840 (2000).
21. Hazeki, N., Tukamoto, T., Goto, J. & Kanazawa, I. Formic acid dissolves aggregates of an N-terminal huntingtin fragment containing an expanded polyglutamine tract: applying to quantification of protein components of the aggregates. *Biochem. Biophys. Res. Commun.* **277,** 386–393 (2000).
22. Moulder, K. L., Onodera, O., Burke, J. R., Strittmatter, W. J. & Johnson, E. M. Jr Generation of neuronal intranuclear inclusions by polyglutamine–GFP: analysis of inclusion clearance and toxicity as a function of polyglutamine length. *J. Neurosci.* **19,** 705–715 (1999).
23. Cummings, C. J. *et al.* Chaperone suppression of aggregation and altered subcellular proteasome localization imply protein misfolding in SCA1. *Nature Genet.* **19,** 148–154 (1998).
24. Bence, N. F., Sampat, R. M. & Kopito, R. R. Impairment of the ubiquitin-proteasome system by protein aggregation. *Science* **292,** 1552–1555 (2001).
25. Hurlbert, M. S. *et al.* Mice transgenic for an expanded CAG repeat in the Huntington's disease gene develop diabetes. *Diabetes* **48,** 649–651 (1999).
26. Farrer, L. A. Diabetes mellitus in Huntington disease. *Clin. Genet.* **27,** 62–67 (1985).
27. Li, H., Li, S. H., Johnston, H., Shelbourne, P. F. & Li, X. J. Amino-terminal fragments of mutant huntingtin show selective accumulation in striatal neurons and synaptic toxicity. *Nature Genet.* **25,** 385–389 (2000).
28. DiFiglia, M. *et al.* Aggregation of huntingtin in neuronal intranuclear inclusions and dystrophic neurites in brain. *Science* **277,** 1990–1993 (1997).
29. Onodera, O. *et al.* Oligomerization of expanded-polyglutamine domain fluorescent fusion proteins in cultured mammalian cells. *Biochem. Biophys. Res. Commun.* **238,** 599–605 (1997).
30. Carter, R. J. *et al.* Characterization of progressive motor deficits in mice transgenic for the human Huntington's disease mutation. *J. Neurosci.* **19,** 3248–3257 (1999).


**Supplementary Information** accompanies the paper on *Nature*'s website (http://www.nature.com/nature).

**Acknowledgements** We thank E. Signer, S. Lokey, M. Kirschner, N. Ayad, M. Kobori, O.Gozani, L. Yoo, R. Sanchez-Olea, A. Degterev and R. King for comments; T. Mitchison for advice; M. Takeuchi for technical assistance; and X.-J. Li, A. Kazantsev and C. Cepko for reagents. This work was supported in part by grants from the Hereditary Disease Foundation and the NIH (to J.Y.).

**Competing interests statement** The authors declare that they have no competing financial interests.

**Correspondence** and requests for materials should be addressed to J.Y. (e-mail: Junying_Yuan@hms.harvard.edu).

# A role for *Drosophila* LKB1 in anterior–posterior axis formation and epithelial polarity

**Sophie G. Martin & Daniel St Johnston**

*The Wellcome Trust/Cancer Research UK Institute and Department of Genetics, University of Cambridge, Tennis Court Road, Cambridge CB2 1QR, UK*

**The PAR-4 and PAR-1 kinases are necessary for the formation of the anterior–posterior (A–P) axis in *Caenorhabditis elegans*[1–3]. PAR-1 is also required for A–P axis determination in *Drosophila*[4,5]. Here we show that the *Drosophila par-4* homologue, *lkb1*, is required for the early A–P polarity of the oocyte, and for the repolarization of the oocyte cytoskeleton that defines the embryonic A–P axis. LKB1 is phosphorylated by PAR-1 *in vitro*, and overexpression of LKB1 partially rescues the *par-1* phenotype. These two kinases therefore function in a conserved pathway for axis formation in flies and worms. *lkb1* mutant clones also disrupt apical–basal epithelial polarity, suggesting a general role in cell polarization. The human homologue, LKB1, is mutated in Peutz–Jeghers syndrome[6,7] and is regulated by prenylation and by phosphorylation by protein kinase A[8,9]. We show that protein kinase A phosphorylates *Drosophila* LKB1 on a conserved site that is important for its activity. Thus, *Drosophila* and human LKB1 may be functional homologues, suggesting that loss of cell polarity may contribute to tumour formation in individuals with Peutz–Jeghers syndrome.**

The A–P axis of *Drosophila* is specified during oogenesis when a signal from the posterior follicle cells induces the formation of a polarized oocyte microtubule cytoskeleton, in which most minus ends are nucleated from the anterior cortex, with the plus ends extending towards the posterior pole[10]. These polarized microtubules direct both the localization of *bicoid* messenger RNA to the anterior of the oocyte to specify where the head and thorax will develop, and the transport of *oskar* mRNA to the posterior, where it induces the formation of polar granules that contain the abdominal and germline determinants[10].